Thermodynamics of Dyadosphere of Reissner-Nordstrom, f(R) Global Monopole and Janis-Newman-Winicour Black Holes

By

Ayesha Sadiq

CIIT/FA14-BSM-013/LHR

BS

In

Mathematics

COMSATS University Islamabad

Lahore Campus

Spring, 2018

COMSATS University Islamabad

Thermodynamics of Dyadosphere of Reissner-Nordstrom, f(R) Global Monopole and Janis-Newman-Winicour Black Holes

A Report Presented to

COMSATS University Islamabad, Lahore Campus

In partial fulfillment

of the requirement for the degree of

BS (Mathematics)

By

Ayesha Sadiq

CIIT/FA14-BSM-013/LHR

Spring, 2018

Thermodynamics of Dyadosphere of Reissner-Nordstrom, f(R) Global Monopole and Janis-Newman-Winicour Black Holes

A Final Year Report is submitted to the Department of Mathematics as partial fulfillment of the requirement for the award of Degree of BS Mathematics.

Name	Registration Number
Ayesha Sadiq	CIIT/FA14-BSM-013/LHR

Supervisor

Dr. Abdul Jawad

Assistant Professor,

Department of

Mathematics

COMSATS University Islamabad, Lahore Campus

Spring 2018

Final Approval

This report titled

Thermodynamics of Dyadosphere of Reissner-Nordstrom, f(R) Global Monopole and Janis-Newman-Winicour Black Holes

By

Ayesha Sadiq

CIIT/FA14-BSMATH-013/LHR

Has been approved

For the COMSATS University Islamabad,Lahore Campus

ExternalExaminer:____________________________

Dr.

Supervisor: _____Dr. Abdul Jawad___

Department of Mathematics /CUI, Lahore Campus

HoD: Dr Sarfraz Ahmad

Department of Mathematics, Lahore Campus

Declaration

I **Ayesha Sadiq** registration number **CIIT/FA14-BSM-013/LHR** hereby declare that I have produced the work presented in this report, during the scheduled period of study.

Date:_______________

____

Ayesha Sadiq

CIIT/FA14-BSM-013/LHR

Certificate

It is certified that **Ayesha Sadiq (CIIT/FA14-BSM-013/LHR)** has carried out all the work related to this report under my supervision at the Department of Mathematics, COMSATS University Islamabad, Lahore Campus, and the work fulfills the requirement for award of BS degree.

Date:__________________

Supervisor:

____

Dr. Abdul Jawad

Assistant Professor

Head of Department:

Dr Sarfraz Ahmad

Associate Professor

Department of Mathematics

DEDICATION

To

My family

Table of Contents

Table of Contents **viii**

List of Figures **x**

Table of Contents **xi**

Acknowledgements **xii**

Abstract **xiii**

1 Introduction **1**

2 Preliminaries **5**

2.1 Fundamental Hypotheses and Postulates of General Relativity 6

2.2 Schwarzschild Line-element 7

2.2.1 Schwarzschild Singularity 14

2.3 Black Hole 15

2.3.1 Singularity 16

2.3.2 Event Horizon 16

2.3.3 Entropy 17

3 Thermodynamics of Dyadosphere of Reissner-Nordström Black Hole **18**

3.1 Dyadosphere of Reissner-Nordström Black Hole 19

3.2 Entropy of Dyadosphere of RN Black Hole 20

3.3 Stability and Phase Transition of Dyadosphere of RN Black Hole 22

3.3.1 Grand Canonical Ensemble 25

3.3.2 Canonical Ensemble 26

4 Thermodynamics of Janis-Newman-Winicour Space-Time and Fragmentation of $f(R)$ Global Monopole **28**
4.1 Janis-Newman-Winicour Space-Time 29
4.1.1 Stability and Phase Transition 30
4.1.2 Grand Canonical Ensemble 33
4.1.3 Canonical Ensemble 34
4.2 The Fragmentation of a Black Hole with a $f(R)$ Global Monopole 35
4.2.1 Stability and Phase Transition 36
4.2.2 Grand Canonical Ensemble 38
4.2.3 Canonical Ensemble 39

5 Conclusion **41**

Bibliography **43**

List of Figures

3.1 Plot of pressure versus horizon radius. 21
3.2 Specific heat at constant volume versus horizon radius. . . . 23
3.3 γ verses horizon radius. 24
3.4 Gibb's free energy in terms of horizon radius. 25
3.5 Helmholtz free energy in terms of horizon radius. 26

4.1 Plot of pressure versus horizon radius. 30
4.2 Specific heat at constant volume versus horizon radius. . . . 31
4.3 γ verses horizon radius. 32
4.4 Gibb's free energy in terms of horizon radius. 33
4.5 Helmholtz free energy in terms of horizon radius. 34
4.6 Plot of pressure versus horizon radius. 36
4.7 Plot of pressure versus horizon radius. 37
4.8 Plot of pressure versus horizon radius. 37
4.9 Plot of pressure versus horizon radius. 39
4.10 Plot of pressure versus horizon radius. 40

Acknowledgements

First of all praises and thanks are for the **Almighty Allah** Who always guides me to the right path and has helped me to complete this thesis work in the given frame of time. Secondly I am thankful to my institution and a special thanks to the Head of Department of Mathematics for providing us with very good research facilities and environment, required for the accomplishment of our goals. I would like to acknowledge my supervisor **Dr. Abdul Jawad** for his guidance, valuable comments and encouragement. I extend my gratitude to Dr. Shamaila Rani for her guidance.

Next, my special thanks to my parents, they have provided me with this great opportunity. Of course, I am indebted to my siblings for their prayers, continuous support and love. Last but not least, I want to thanks a lot to faculty members of my department of mathematics, my class fellows and my friends.

Lahore **Ayesha Sadiq**

25 May, 2018

Abstract

In this thesis, we study the effects of thermal fluctuations on Dyadosphere of Reissner-Nordström, Janis-Newman-Winicour and the fragmentation of $f(R)$ global monopole black holes. In the presence of these fluctuations, we obtain various thermodynamic quantities like entropy, pressure, specific heat, Gibb's free energy and Helmholtz free energy. We discuss the stability of these black holes using the γ (the ratio of heat capacities). We also discuss the phase transition, grand canonical ensemble and canonical ensemble. It is demonstrated that in Dyadoshpere of Reissner-Nordström, Janis-Newman-Winicour and fragmentation of $f(R)$ global monopole black holes become locally and globally stable with respect to increasing value of horizon radius.

Chapter 1

Introduction

The black hole solution is one of the most important topics in general relativity. It is an open problem to understand the inner nature of black hole (BH). The BH is first predicted by Einstein in 1916, with his theory of general relativity and was first discovered in 1971. Because of Bekenstein-Hawking entropy and Hawking temperature BH behaves as thermodynamics objects [1]-[7], and because the existence of horizon deep connection exists between the laws of classical general relativity, thermodynamics and quantum mechanics [1]-[10]. According to the second law of thermodynamics objects, if an entropy was not associated with a BH then this law is violated. This happens whenever entropy of BH is absent and cause a spontaneous reduction in entropy of the universe.

black holes are objects of maximum entropy. Objects are of the same volume have less entropy than BHs [11, 12]. This entropy is proportional to the area of BH [13] .This entropy is determined by $S = \frac{A}{4}$, where S represent the entropy of matter outside BH and A represent the surface area of event horizon. Importance of quantum fluctuation occur when BH contract its size , due to this entropy of BH it required to be corrected,and expected from this to modify the holographic principle [14, 15]. As the BH reduce it's size because of hawking radiations, quantum fluctuation required to correct the relation between area and the entropy of BH.

To evaluate these corrections there are many approaches, one is non-perturbative quantum general relativity [16]. It was showed that the leading order relation between entropy and area of BH is Bekenstein entropy-area relation. This pattern also given logarithmic correction terms to the Bekenstein entropy-area relation. Cardy formula has also been showed that logarithmic correction terms should take place in all BHs whose microscopic degree of freedom are described by a conformal field theory [17, 18]. In the presence of BH, matter field have also been studied, and this study has also generated logarithmic correction terms for the Bekenstein entropy-area formula [19]-[21]. By evaluating exact partition function these logarithmic corrections have been obtained for three-dimensional BTZ BH [22]. To obtain logarithmic correction to the entropy of a BH Rademacher expansion of the partition function also has been used [23].

The vacuum mimetic $f(R)$ gravity with Lagrange multiplier and mimetic scalar potential have solution by the conditions of Reissner-nordstron(RN) anti-de sitter BH [24]. The thermal interpretation of the Schwinger effect for charged scalars and spinors in an extremal and near-extremal RN BH [25]. Thermodynamics method is the statement of RN BHs in arbitrary dimensions [26].

In general theory of relativity the gravitational divergence of light ray is a considerable prediction. In Janis-Newman-Winicour (JNW) geometry the gravitational deflection increases with charge and decreases with the charge in RN geometry [27]. We obtain the calculations for Kerr BH and JNW solution, that have naked singularity on surface at finite radius [28]. The geodesic formation of JNW space-time obtain a strong curvature naked singularity [29]. The thermodynamic quantities are explore as the local temperature, heat capacity, free energy and the stability of BH include a global monopole within or outside the $f(R)$ gravity [30]. The Chen and Cheng also work on $f(R)$ global monopole [31]. Because the entropy difference is negative the $f(R)$ global monopole BH remains stable instead of splitting without the generalization [32].

Thermal stability of BH is the most important thermodynamical quantities. BHs should stable in dynamics and thermodynamics models because of their physical nature. The instability of BH is that it may have a phase transition or if it is completely unphysical. In the present thesis, the organization of thesis is as follows:

i) Some basic definitions and mathematical formulae are given to understand the thesis work in nxt chapter.

ii) In Chapter **2**, we consider RNBH and check the thermodynamic quantities like entropy, pressure, specific heat, Gibb's free energy and Helmholtz free energy in the presence of thermal fluctuation. We check the stability of BH. We also discuss the phase transition of BH and discuss the local and global stability of BH.

iii) Chapter **3** represents the thermodynamics of Janis-Newman-Winicour space-time and fragmentation of $f(r)$ global monopole. we consider RNBH and check the thermodynamic quantities like entropy, pressure, specific heat, Gibb's free energy and Helmholtz free energy in the presence of thermal fluctuation. We check the stability of BH. We also discuss the phase transition of BH and discuss the local and global stability of BH.

iv) The last chapter contains the summary of the results.

Chapter 2

Preliminaries

This chapter has the basic concepts to understand the thesis work.

2.1 Fundamental Hypotheses and Postulates of General Relativity

General relativity is based on the following set of fundamental principle, which guided its development. These are in the following:

1. The general principle of relativity-The laws of physics must be the same for all observers (accelerated or not).

2. Physical events are described in a four-dimensional space-time manifold, the metric of which is

$$ds^2 = g_{\mu\nu} dx^\mu dx^\nu, \tag{2.1.1}$$

3. Principle of covariance: The laws of physics must take the same form in all coordinates systems.

4. Local Lorentz invariance: The laws of special relativity apply locally for all inertial observers.

5. The principle that inertial motion is geodesic motion. The world lines of particles unaffected by physical forces are time-like or null geodesic of space-time.

6. Space-time is curved. This permits gravitational effects, such as free fall to be described as a form of inertial motion.

7. Space-time curvature is created by stress-energy within the space-time. This is described in general relativity by Einstein's field equations, which in the presence of matter are

$$R_{\mu\nu} - \frac{1}{2} g_{\mu\nu} R + \Lambda_{\mu\nu} = -\kappa T_{\mu\nu}, \tag{2.1.2}$$

where $T_{\mu\nu}$ is the energy-momentum tensor and we express this energy-momentum tensor

$$T_{\mu\nu} = (\rho + p)u_\mu u_\nu \pm p g_{\mu\nu}, \tag{2.1.3}$$

Or

$$T^{\mu\nu} = (\rho + p)u^\mu u^\nu \pm p g^{\mu\nu}. \tag{2.1.4}$$

In empty space, $T^{\mu\nu} = 0$, and the equation becomes

$$R_{\mu\nu} = 0. \tag{2.1.5}$$

The equivalent principle, which served as a starting point for the development of general relativity, ended up being a consequence of general principle of relativity and the principle that inertial motion is geodesic motion.

2.2 Schwarzschild Line-element

It is intended to find a line-element for an interval in the vicinity of a gravitating point particle, for instance, the sun. In the empty space, the spacetime would be flat and in spherical polar coordinates and time, the line element is given by

$$ds^2 = dt^2 - dr^2 - r^2 d\theta^2 - r^2 \sin^2\theta d\phi^2. \tag{2.2.1}$$

In this equation, the velocity of light c is taken to be unity in order to use relativistic units. The isolated particle is assumed to be static and spherically symmetrical and hence, the gravitational field will depend on r alone and not on θ, ϕ. The line-element would be spatially spherically symmetric about the point and static. Thus, the line-element in the most general form is

$$ds^2 = -e^\lambda dr^2 - r^2(d\theta^2 + \sin^2\theta d\phi^2) + e^\nu dt^2, \tag{2.2.2}$$

where $\lambda = \lambda(r)$ and $\nu = \nu(r)$. However, the gravitational field due to the particle decreases as we move away from it and the line-element, Eq.(2.2.2) will become the Galilean line-element at $r = \infty$. Thus, $\lambda = 0 = \nu$ at $r = \infty$.

Rewriting the line-element, Eq.(2.2.2) as

$$ds^2 = g_{\mu\nu} dx^\mu dx^\nu, \tag{2.2.3}$$

with $x^0 = t$, $x^1 = r$, $x^2 = \theta$, $x^3 = \phi$. The metric tensor $g_{\mu\nu}$ is

$$g_{\mu\nu} = \begin{pmatrix} e^\nu & 0 & 0 & 0 \\ 0 & -e^\lambda & 0 & 0 \\ 0 & 0 & -r^2 & 0 \\ 0 & 0 & 0 & -r^2\sin^2\theta \end{pmatrix} \tag{2.2.4}$$

The inverse metric tensor $g^{\mu\nu}$ is

$$g^{\mu\nu} = \begin{pmatrix} e^{-\nu} & 0 & 0 & 0 \\ 0 & -e^{-\lambda} & 0 & 0 \\ 0 & 0 & -r^{-2} & 0 \\ 0 & 0 & 0 & \frac{-1}{r^2\sin^2\theta} \end{pmatrix} \tag{2.2.5}$$

Let us evaluate the Christoffels $3 - index$ symbols $\Gamma^\alpha_{\mu\nu}$, $\Gamma_{\alpha,\mu\nu}$ for the static and spherically symmetric line-element, Eq.(2.2.3). Recalling that

$$\Gamma_{\alpha,\mu\nu} = \frac{1}{2(\partial_\nu g_{\alpha\mu} + \partial_\mu g_{\alpha\nu} - \partial_\alpha g_{\mu\nu})}, \tag{2.2.6}$$

$$\Gamma^\alpha_{\mu\nu} = g^{\alpha\lambda}\Gamma_{\lambda,\mu\nu}. \tag{2.2.7}$$

In view of the symmetry relation, Eq.(2.2.6), only 40 are independent out of the 64 $3 - index$ symbols. In addition, for the line-element, Eq.(2.2.3), 31Christoffels $3-index$ symbols are zero and the following nine are non-zero. Further, it is clear that since $g_{\mu\nu}$ is diagonal, the $3-index$ symbols with all the three indices different, are zero.

$$\begin{aligned}
\Gamma^0_{10} &= \frac{1}{2}v', \quad \Gamma^2_{12} = \frac{1}{r}, \\
\Gamma^1_{00} &= \frac{1}{2}v'e^{v-\lambda}, \quad \Gamma^2_{33} = -r\sin\theta\cos\theta, \\
\Gamma^1_{11} &= \frac{1}{2}\lambda', \quad \Gamma^3_{13} = \frac{1}{r}, \\
\Gamma^1_{22} &= -re^{-\lambda}, \quad \Gamma^3_{32} = \cot\theta \\
\Gamma^1_{23} &= -r\sin^2\theta e^{-\lambda},
\end{aligned} \tag{2.2.8}$$

where $\nu' = \frac{dv}{dr}$ and $\lambda' = \frac{d\lambda}{dr}$. Einsteins law of gravitation for empty space is

$$R_{\mu\nu} = 0, \tag{2.2.9}$$

where $R_{\mu\nu}$ is the contracted curvature tensor. Making use of the $3-index$ symbols Equation Eq.(2.2.8), we calculate the different components of $R_{\mu\nu}$, given by

$$R_{\mu\nu} = -\partial_\alpha\Gamma^\alpha_{\mu\nu} + \partial_\nu\Gamma^\alpha_{\mu\alpha} + \Gamma^\rho_{\mu\alpha}\Gamma^\alpha_{\nu\rho} - \Gamma^\alpha_{\mu\nu}\Gamma^\rho_{\alpha\rho}, \tag{2.2.10}$$

Thus

$$\begin{aligned}
R_{00} =& -\partial_\alpha\Gamma^\alpha_{00} + \Gamma^\rho_{0\alpha}\Gamma^\alpha_{0\rho} - \Gamma^\alpha_{00}\Gamma^\rho_{\alpha\rho} \\
=& -\partial_1\Gamma^1_{00}\Gamma^0_{01} + \Gamma^0_{01}\Gamma^1_{00} - \Gamma^1_{00}(\Gamma^0_{10} + \Gamma^1_{11} + \Gamma^2_{12} + \Gamma^3_{13}) \\
=& -\partial_1(\frac{1}{2}v'e^{v-\lambda}) + 2\frac{1}{4}v'^2e^{v-\lambda} - \frac{1}{2}v'e^{v-\lambda}\left(\frac{1}{2}v' + \frac{1}{2}\lambda' + \frac{2}{r}\right) \\
=& -\frac{1}{2}[v''v'(v'-\lambda')]e^{v-\lambda} + \frac{1}{2}v'^2e^{v-\lambda} - \frac{1}{4}v'e^{v-\lambda}(v'+\lambda') - \frac{v'}{r}e^{v-\lambda}.
\end{aligned} \tag{2.2.11}$$

Analogously, we calculate $R_1 1$.

$$
\begin{aligned}
R_{11} =& - \partial_\alpha \Gamma^\alpha_{11} + \partial_1 \Gamma^\alpha_{1\alpha} + \Gamma^\rho_{1\alpha}\Gamma^\alpha_{1\rho} - \Gamma^\alpha_{11}\Gamma^\rho_{\alpha\rho} \qquad (2.2.12)\\
=& - \partial_1 \Gamma^1_{11} + \partial_1 \Gamma^0_{10} + \partial_1 \Gamma^1_{11} + \partial_1 \Gamma^2_{12} + \partial_1 \Gamma^3_{13} + \Gamma^0_{1\alpha}\Gamma^\alpha_{10}\\
&+\Gamma^1_{1\alpha}\Gamma^\alpha_{11} + \Gamma^2_{1\alpha}\Gamma^\alpha_{12} + \Gamma^3_{1\alpha}\Gamma^\alpha_{13} - \Gamma^1_{11}(\Gamma^0_{10} + \Gamma^1_{11} + \Gamma^2_{12} + \Gamma^3_{13})\\
=&\partial_1(\Gamma^1_{11} + \Gamma^2_{12} + \Gamma^3_{13}) + \Gamma^0_{10}\Gamma^0_{10} + \Gamma^1_{11}\Gamma^1_{11} + \Gamma^2_{12}\Gamma^2_{12} + \Gamma^3_{13}\Gamma^3_{13}\\
&-\Gamma^1_{11}(\Gamma^0_{10} + \Gamma^1_{11} + \Gamma^2_{12} + \Gamma^3_{13})\\
=&\partial_1\left(\frac{1}{2\nu'} + \frac{2}{r}\right) + \frac{\nu'^2}{4} + \frac{\lambda'^2}{4} + \frac{2}{r^2} - \frac{\lambda'}{2}\left(\frac{\nu'}{2} + \frac{\lambda'}{2} + \frac{2}{r}\right)\\
R_{11} =&\frac{1}{2}\nu'' + \frac{1}{4}\nu'^2 - \frac{1}{4}\nu'\lambda' - \frac{\lambda'}{r}.
\end{aligned}
$$

Similarly,we calculate R_{22}

$$
\begin{aligned}
R_{22} =& - \partial_\alpha \Gamma^\alpha_{22} + \partial_2 \Gamma^\alpha_{2\alpha} + \Gamma^\rho_{2\alpha}\Gamma^\alpha_{2\rho} - \Gamma^\alpha_{22}\Gamma^\rho_{\alpha\rho} \qquad (2.2.13)\\
=& - \partial_1 \Gamma^1_{22} + \partial_2 \Gamma^3_{23} + \Gamma^\rho_{2\alpha}\Gamma^1_{2\rho} + \Gamma^\rho_{22}\Gamma^2_{2\rho} + \Gamma^\rho_{23}\Gamma^3_{2\rho}\\
&-\Gamma^1_{22}(\Gamma^0_{10} + \Gamma^1_{11} + \Gamma^2_{12} + \Gamma^3_{13})\\
=&\partial_1(-re^{-\lambda}) + \partial_2(cot\theta) + \Gamma^2_{21}\Gamma^1_{22} + \Gamma^1_{22}\Gamma^2_{21} + \Gamma^3_{23}\Gamma^3_{23}\\
&+re^{-\lambda}(\frac{1}{2\nu'} + \frac{1}{2\lambda'} + \frac{2}{r})\\
=&e^{-\lambda} - r\lambda' e^{-\lambda} - \csc^2\theta - 2e^{-\lambda} + \cot^2\theta\\
&+re^{-\lambda}(\frac{1}{2\nu'} + \frac{1}{2\lambda'} + \frac{2}{r}).
\end{aligned}
$$

Lastly we calculate R_{33}.

$$
\begin{aligned}
R_{33} =& -\partial_\alpha \Gamma^\alpha_{33} + \partial_3 \Gamma^\alpha_{3\alpha} + \Gamma^\rho_{3\alpha}\Gamma^\alpha_{3\rho} - \Gamma^\alpha_{33}\Gamma^\rho_{3\rho} \\
=& -\partial_1 \Gamma^1_{33} + \partial_2 \Gamma^2_{33} + \Gamma^\rho_{31}\Gamma^1_{3\rho} + \Gamma^\rho_{32}\Gamma^2_{3\rho} + \Gamma^\rho_{33}\Gamma^3_{3\rho} \\
& -\Gamma^1_{33}\big(\Gamma^0_{10} + \Gamma^1_{11} + \Gamma^2_{12} + \Gamma^3_{13}\big) - \Gamma^2_{33}\big(\Gamma^3_{23}\big) \\
=& -\partial_1(-r\sin^2\theta e^{-\lambda}) - \partial_2(-\sin\theta\cos\theta) + \Gamma^3_{13} + \Gamma^1_{33} + \Gamma^3_{23} + \Gamma^2_{33} \\
& +\Gamma^1_{33}\Gamma^3_{31} + \Gamma^2_{33}\Gamma^3_{32} - \Gamma^1_{33}(\frac{\nu'}{2} + \frac{\lambda'}{2} + \frac{2}{r}) - \Gamma^2_{33}(\cot\theta) \\
=& \sin^2\theta e^{-\lambda} - r\lambda'\sin^2\theta e^{-\lambda} + \cos 2\theta + 2(-\sin^2\theta e^{-\lambda} - \cot\theta\sin\theta\cos\theta) \\
& +r\sin^2\vartheta e^{-\lambda}(\frac{\nu'}{2} + \frac{\lambda'}{2} + \frac{2}{r}) + \sin\theta\cos\theta\cot\theta \\
=& \sin^2\theta e^{-\lambda}(1 - r\lambda') + \cos 2\theta + \frac{1}{2r}\sin^2\theta e^{-\lambda}(\nu' + \lambda') \\
& +2\sin^2\theta e^{-\lambda} - 2\sin^2\theta e^{-\lambda} - 2\cos^2\theta + \cos^{2\theta} \\
=& \sin^2\theta e^{-\lambda}\big[1 + \frac{1}{2r\nu'} - \frac{1}{2r\lambda'}\big] + \cos 2\theta - \cos^2\theta \\
=& \sin^2\theta e^{-\lambda}\big[1 + \frac{1}{2r\nu'} - \frac{1}{2r\lambda'}\big] - \sin^2\theta. \qquad (2.2.14)
\end{aligned}
$$

Also

$$R_{33} = \sin^2\theta R_{22} \qquad (2.2.15)$$

We summarized the final form of components as

$$
\begin{aligned}
R_{00} =& -\frac{1}{2e^{\nu-\lambda}}(\nu'' + \frac{1}{2\nu'^2} - \frac{1}{2\nu'\lambda'} + \frac{2\nu'}{r}), \\
R_{11} =& \frac{1}{2\nu''} + \frac{1}{4\nu'^2} + \frac{1}{4\nu'\lambda'} - \frac{\lambda'}{r}, \\
R_{22} =& e^{-\lambda}(1 + \frac{1}{2r\nu'} - \frac{1}{2r\lambda'}) - 1, \\
R_{33} =& \sin^2\theta R^{22}. \qquad (2.2.16)
\end{aligned}
$$

Now the field Eq.(2.2.9) becomes using Eq.(2.2.16) as

$$e^{-\lambda}(\nu'' + (\frac{1}{2})\nu'^2 - (\frac{1}{2})\nu'\lambda' + \frac{2\nu'}{r}) = 0, \tag{2.2.17}$$

$$\frac{\nu''}{2} + \frac{\nu'^2}{4} - \frac{\nu'\lambda'}{4} - \frac{\lambda'}{r} = 0, \tag{2.2.18}$$

$$e^{-\lambda}(1 + \frac{1}{2r\nu'} - \frac{1}{2r\lambda'}) - 1 = 0, \tag{2.2.19}$$

$$\left[e^{-\lambda}(1 + \frac{1}{2r(\nu' - \lambda'})) - 1\right]\sin^2\theta = 0. \tag{2.2.20}$$

Obviously, Eq.(2.2.19) and Eq.(2.2.20) are identical. The three independent Eqs.(2.2.17), (2.2.18) and (2.2.19) enable us to determine the unknown functions ν and λ. Dividing Eq.(2.2.17) by $e^{-\lambda}$, we obtain

$$\nu'' + \frac{1}{2\nu'^2} - \frac{1}{2\nu'\lambda'} + \frac{2\lambda'}{r} = 0. \tag{2.2.21}$$

Rewriting Eq.(2.2.18), we get

$$\nu'' + \frac{\nu'}{2} - \frac{\nu'\lambda'}{2} - \frac{2\lambda'}{r} = 0. \tag{2.2.22}$$

Subtracting Eq.(2.2.22) from Eq.(2.2.21), we get

$$\frac{2}{r(\nu' + \lambda')} = 0. \tag{2.2.23}$$

Integrating Eq.(2.2.23), we obtain

$$\nu + \lambda = C, \tag{2.2.24}$$

where C is a constant of integration. The gravitational field (disturbance from flat space-time) due to the particle, diminishes as we record to the infinite distance. It implies that the line-element, Eq.(2.2.2), must assume the form of Galilean line-element at $r = \infty$. Thus, we must take $\nu = 0 = \lambda$ at $r = \infty$. Thus, $C = 0$ in Eq.(2.2.24). Therefore,

$$\nu + \lambda = 0 \tag{2.2.25}$$

or $\nu = -\lambda$ In view of Eq.(2.2.25), the Eq.(2.2.19) becomes

$$e^{-\lambda}(1 - r\lambda') - 1 = 0, \tag{2.2.26}$$

$$\frac{d}{dr}(re^{-\lambda}) = 1, \tag{2.2.27}$$

$$re^{-\lambda} = r + C_1, \tag{2.2.28}$$

$$e^{-\lambda} = 1 + \frac{C_1}{r}. \tag{2.2.29}$$

putting $C_1 = -2m$, we get

$$e^{\nu} = e^{-\lambda} = 1 - \frac{2m}{r}. \tag{2.2.30}$$

The constant of integration is put equal to $-2m$, in order to facilitate the physical interpretation of m as the mass of gravitating particle. The line-element. Eq.(2.2.2), due to static, isolated gravitating mass point is, in relativistic units $(c = G = 1)$

$$ds^2 = \left(1 - \frac{2m}{r}\right)dt^2 - \left(1 - \frac{2m}{r}\right)^{-1} dr^2 - r^2(d\theta^2 + \sin^2\theta . d\phi) \tag{2.2.31}$$

In c.g.s. units, if the mass is M, the line-element is

$$ds^2 = \left(1 - \frac{2MG}{rc^2}\right)dt^2 - \left(1 - \frac{2MG}{rc^2}\right)^{-1} dr^2 - r^2(d\theta^2 + \sin^2\theta d\phi). \tag{2.2.32}$$

As it was obtained first by Schwarzschild in the closed form, it is called Schwarzschilds exterior solution. As is obvious, in the limit $r \to \infty$, it goes over to the metric of spacetime of special relativity. This solution is of fundamental importance. We included the cosmological constant Λ, then for empty space, the solution corresponding to the field equations

$$R_{\mu\nu} = \Lambda g_{\mu\nu}, \tag{2.2.33}$$

can be obtained by taking $T_{\mu\nu} = 0$ and the resulting metric is

$$ds^2 = \left(1 - \frac{2m}{r} - \frac{\Lambda r^2}{3}\right)dt^2 - \left(1 - \frac{2m}{r} - \frac{\Lambda r^2}{3}\right)^{-1} dr^2 - r^2(d\theta^2 + \sin^2\theta d\phi^2). \tag{2.2.34}$$

Comparing the two metrics, Eq.(2.2.31) and Eq.(2.2.34), we see that the effect of term Λ on the field surrounding the attracting particle, increases with r, i.e., the size of the region considered. But as we will see in the next section, the motion of planets is described with great accuracy by Eq.(2.2.32), we infer that the cosmological constant Λ, is so small that it does not produce tangible effects within regions of the size comparable to the solar system.

2.2.1 Schwarzschild Singularity

Schwarzschild solution, Eq.(2.2.31) has the following singularities:

- $r = 0$. But this type of singularity is usual and also occurs in the Newtonian theory of gravitation.

- $r = 2m$. The value of r is called the **Schwarzschilds radius**. At $r = 2m$, g_{00} becomes zero and g_{11} becomes infinite. For points $0 \leq r \leq 2m$, $ds^2 < 0$, i.e., the interval is purely space-like.

Let us estimate the singular region for the sun. If it has the radius r, then

$$r = 2m = \frac{2mG}{c^2} = 2.956. \tag{2.2.35}$$

The physical radius of sun is $6.960105km$, thus, the singular region is extreme deeply embedded in it. For a region inside, the Schwarzschild solution of Einsteins field equations, does not hold as $T_{\mu\nu}$ will not be zero. This is the situation long before the singular region starts. The Schwarzschilds radius is always much smaller than the physical radius of the body, say earth, electron.

However, it may be noted that Einstein and Rosen have shown that the singularity in the Schwarzschild solution, Eq.(2.2.31), can be removed by the transformation

$$r - 2m = u^2 \tag{2.2.36}$$

The line-element, Eq.(2.2.31), then becomes

$$ds^2 = -4(u^2 + 2m)du^2 - (u^2 + 2m)^2(d\theta^2 + \sin^2\theta d\phi^2) + \frac{u^2}{u^2 + 2m} \tag{2.2.37}$$

The singularity is no more there in the line-element, but the singularity $r = 2m$ has been shifted from the line-element, Eq.(2.2.31) to the transformation, Eq.(2.2.36). The Jacobian of this transformation is zero at $u = 0$. But in general relativity, only non-singular transformations are allowed so that the Jacobian has to be non-zero and finite within its domain. Furthermore, the line-element, Eq.(2.2.37), is free of singularity only if m is positive, implying thereby that only positive values of mass are permissible. However, this is only a tentative argument.

2.3 Black Hole

Black hole represents an infinitely dense object whose gravitational force is so strong that anything (matter and radiation) cannot escape from its gravitational field. It is produced through the process of gravitational col lapse in which the massive objects or stars collapse under their own gravity and form an object with infinite density. It is impossible to analyze inside of the BH by naked eyes as light cannot reflect back from it due to its strong gravitational force. However, it can be detected by its effects on neighboring celestial objects.

Generally, a BH is characterized by its mass, charge and angular momentum (spin). The simplest BH is the Schwarzschild BH that has no charge and spin. The example of BH which has both mass as well as charge is called Reissner Nordstrom (RN) BH while the Kerr BH has both mass and spin. The BH which has all the parameters, i.e., mass, charge and spin is called Kerr-Newman BH.

2.3.1 Singularity

Singularity indicates the location where gravitational field measuring quantities, i.e., scalar invariant curvature of spacetime, are independent of co ordinate system and become infinite. In BH, this is the point at its center where spacetime does not exist and matter is compressed to in?nite density. There are generally two types of singularity:

True singularity: It is the point in spacetime where all physical laws be come invalid. It is also known as essential singularity and is non-removable.

Coordinate singularity: The coordinate or removable singularity can be removed by a suitable coordinate transformations.

2.3.2 Event Horizon

Event horizon is the boundary of space time beyond which events cannot be observed by any external observer. It is a boundary around the singularity that encloses the BH. Anything (even light) may fall into it but cannot escape back.

2.3.3 Entropy

The entropy of black hole is one fourth of the event horizon. Hawking proposed the famous formula of entropy

$$S = \frac{A}{4}. \tag{2.3.1}$$

where A represent area of event horizon.

Chapter 3

Thermodynamics of Dyadosphere of Reissner-Nordström Black Hole

In this chapter, we consider RNBH and check the thermodynamic quantities like entropy, pressure, specific heat, Gibb's free energy and Helmholtz free energy in the presence of thermal fluctuation. We check the stability of BH. We also discuss the phase transition of BH and discuss the local and global stability of BH.

3.1 Dyadosphere of Reissner-Nordström Black Hole

Dyadosphere of Reissner-Nordström (DSRN) metric is the solution of the Einstein field equation. It draws the space time geometry around a spherically non-rotating charged BH. Large part of the universe appear electrically neutral, so it is unlikely to found a macroscopic objects that have a large amount of net charge. Therefore, DSRN solution is not relevant to realistic solution in astrophysics. However, it contributed in understanding the fundamental nature of space and time. The geometry for static and spherically symmetric solution is

$$ds^2 = A(r)dt^2 - A^{-1}(r)dr^2 - r^2 d\theta^2 - r^2 \sin^2\theta d\varphi^2, \tag{3.1.1}$$

where $A(r)$ is determined by field equations. We have expression for $A(r)$ is

$$A(r) = 1 - \frac{2m}{r} + \frac{\kappa Q^2}{2r^2} - \frac{\kappa\alpha Q^4}{5r^6}, \tag{3.1.2}$$

where m is the mass, Q represents the charge, α is an arbitrary constant and κ is the Newtonian constant and it's formula is $\kappa = \frac{8\pi G}{c^4}$. Solving Eq. (3.1.2), by putting $A(r) = 0$, we get

$$m = \frac{10r^6 + 5\kappa Q^2 r^4 - 2\kappa\alpha Q^4}{20r^5}, \tag{3.1.3}$$

which implies that $r \neq 0$. The entropy of DSRN which associated with the area of BH horizon is $S_0 = \pi r^2$ and the volume is

$$V = \frac{4}{3}\pi r^3. \tag{3.1.4}$$

Temperature of RN is defined as

$$T = \frac{A'(r)}{4\pi} = \frac{10r^6 - 5\kappa Q^2 r^4 + 10\kappa\alpha Q^4}{40\pi r^7}. \tag{3.1.5}$$

3.2 Entropy of Dyadosphere of RN Black Hole

The correction entropy can be written as

$$S = S_0 - \frac{1}{2}\ln S_0 T^2. \tag{3.2.1}$$

In the geometry of a BH quantum fluctuation give rise to the important problem of thermal fluctuation in thermodynamics of BH. So it is sufficient to contribute this correction term when size of BH is small and its temperature is large. Hence, we can avoid the quantum fluctuation to the geometry of large BH. It is obvious that thermal fluctuation only become significant for BH having large temperature and size of BH reduces as its temperature increases. Hence, we can conclude that this correction term will only contribute when the size of BH is sufficiently small.

$$S = S_0 - \frac{b}{2}\ln(S_0 T^2).$$

Thus, we added the parameter b to handle the logarithmic correction terms coming from thermal fluctuations. By setting $b = 1$ one can recover expression for entropy without any correction. So for large BH whose temperature

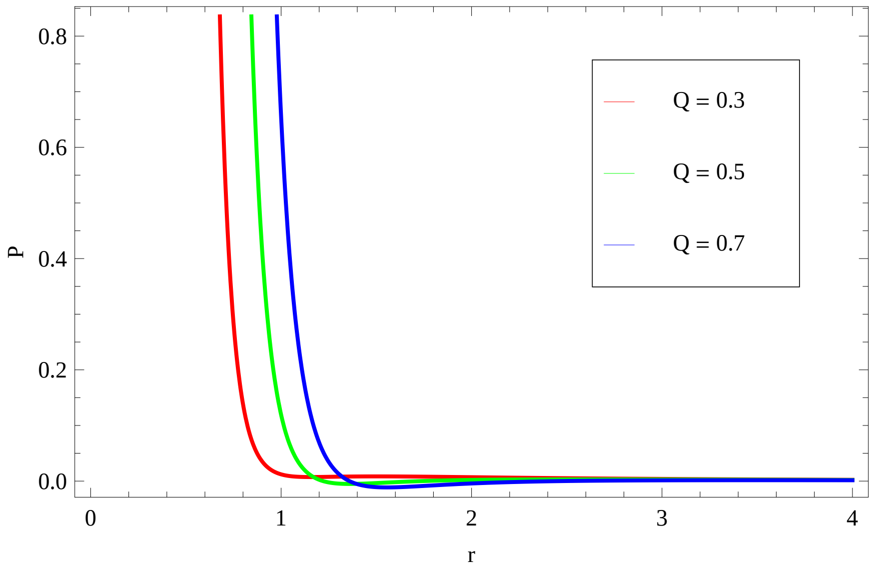

Figure 3.1: Plot of pressure versus horizon radius.

is small, one can take limit $b \to 0$. We can obtain the following entropy

$$S = \pi r^2 - \frac{b}{2}\ln\frac{(10r^6 - 5\kappa Q^2 r^4 + 10\kappa\alpha Q^2)^2}{(40)^2\pi r^{12}}. \tag{3.2.2}$$

It is clear that in the presence of logarithmic correction entropy of BH decreases. We can calculate the value of pressure by using Eqs. (3.1.4), (3.1.5), (3.2.2) which is

$$\begin{aligned} P &= T\left(\frac{\partial S}{\partial V}\right)_V \\ &= \frac{10\pi^2(2r^6 - \kappa Q^2 r^4 + 2\kappa\alpha Q^2) - 10\kappa Q^2 r^4 b + 60\kappa\alpha Q^4 b}{160\pi^2 r^{10}}. \end{aligned} \tag{3.2.3}$$

In the **Fig.3.1**, we discuss the behavior of pressure for three values of charge Q by taking $b = 1$, $\kappa = 8\pi$ and $\alpha = 2$. We see that the value of pressure first increases but after then it decreases. We see that due to logarithmic correction value of pressure decreases. Pressure decreases when the value of radius horizon increases. When $r = 1.6$ the pressure approaches to zero but at $r = 1.8$ pressure increases. For $r > 2$ the value of pressure remains constant.

3.3 Stability and Phase Transition of Dyadosphere of RN Black Hole

In this section, we analyze the thermodynamic stability of DSRN due to the effect of thermal fluctuations. An important measurable physical quantity in BH thermodynamics is thermal capacity or heat capacity. It recognizes the amount of heat required to change the temperature of BH. The stability or instability of BH depends on the nature of heat capacity. If heat capacity is positive then the black hole is stable, and divergence of heat capacity shows phase transition.

- C_P: measure the heat capacity when heat is added to the system under constant pressure.
- C_V: measure the heat capacity when heat is added to the system under constant volume.

We obtain the specific heat under constant volume by using the Eqs. (3.1.5) and (3.2.2)

$$\begin{aligned} C_V &= T\left(\frac{\partial S}{\partial T}\right)_V \\ C_V &= \frac{4\pi r^8 - 2\kappa Q^2 r^4 b + 12\kappa\alpha Q^4 b + 4\kappa\alpha Q^4 \pi r^2 - 2\kappa Q^2 r^6 \pi}{-2r^6 + 3\kappa Q^2 r^4 - 14\kappa Q^4 \alpha}. \end{aligned} \tag{3.3.1}$$

We can find the thermodynamical stability of the BH is to determine the sign of specific heat. The BH is locally stable for $C_V > 0$. We can find the point of the phase transition at $C_V = 0$ and BH is locally unstable for $C_V < 0$.From the **Fig.3.2** we observe that when $Q = 0.5$ then the horizon radius for local stability is $1.3 < r < 2.7$, when $Q = 0.7$ the horizon radius for local stability is $2.7 < r < 3.7$ and for $Q = 0.3$ the horizon radius for

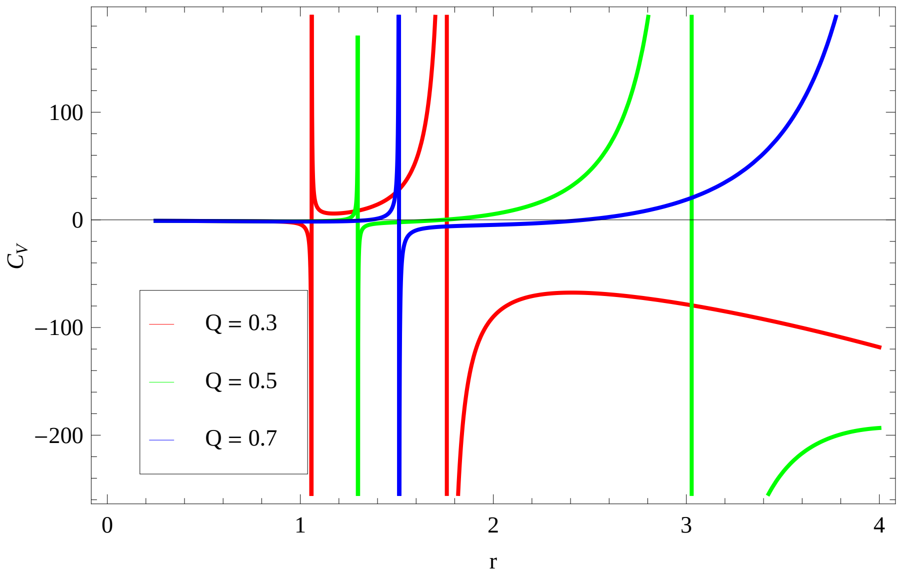

Figure 3.2: Specific heat at constant volume versus horizon radius.

local stability is $1.1 < r < 1.7$. When $Q = 0.3$ the horizon radius for locally unstable is $1.8 < r < 4$ and for $Q = 0.5$ the horizon radius is $3.4 < r < 4$. Now we can find the critical point of the phase transition. The critical point for $Q = 0.7$ is $r = 1.5$ and 2.2. The critical point for $Q = 0.5$ is $r = 1.3$ and critical point for $Q = 0.3$ is $r = 0.9$. We notice that phase transition of $Q = 0.3$ is near to BH as compare to $Q = 0.5$ and $Q = 0.7$. Hence, we can conclude that if we increase the value of Q the phase transition gets shifted towards BH.

The specific heat under constant pressure can be obtained by using the value of M and T as

$$\begin{aligned} C_P &= \left(\frac{\partial M}{\partial T}\right)_P \\ C_P &= \frac{2\pi r^2(-2r^6 + Q^2 r^4\kappa - 2Q^4\alpha\kappa)}{2r^6 - 3Q^4 r^4\kappa + 14Q^4\alpha\kappa}. \end{aligned} \tag{3.3.2}$$

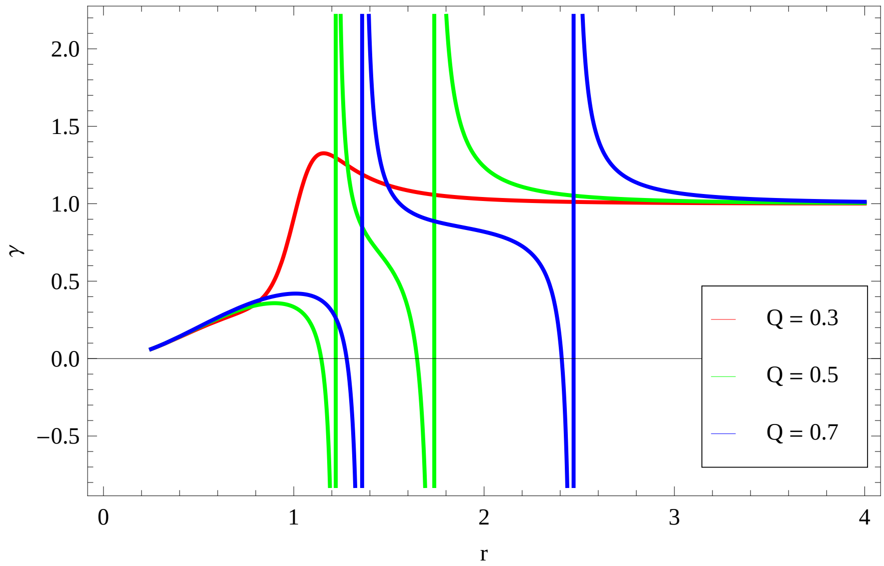

Figure 3.3: γ verses horizon radius.

Using Eqs.(3.3.1) and (3.3.2), we get

$$\gamma = \frac{C_P}{C_V} \tag{3.3.3}$$

$$\gamma = \frac{\pi r^2(2r^6 - Q^2 r^4 \kappa + 2Q^4 \alpha\kappa)}{2\pi r^8 + Q^2(-r^4(b + \pi r^2) + 2Q^2(3b + \pi r^2)\alpha)\kappa}. \tag{3.3.4}$$

We can determine the value of γ by using this expression $\gamma = C_P/C_V$. From **Fig.3.3** we observe that the value of γ decreases due to logarithmic corrections. We obtain the maximum value of γ for $Q = 0.3$ and $\gamma \to 1.4$ when $r = 1.2$. We note that $\gamma \to 1.3$ when $Q = 0.5, 0.7$ for large horizon. We can see that the value of γ approaches to zero at $r = 0.2$ for $Q = 0.3, 0.5$ and 0.7. We observe that the value of γ is stable for $r > 1.2$. As the value of r increasing the value of γ become constant. It is interesting to note that the value of γ show a unstable behavior for $r < 0.8$.

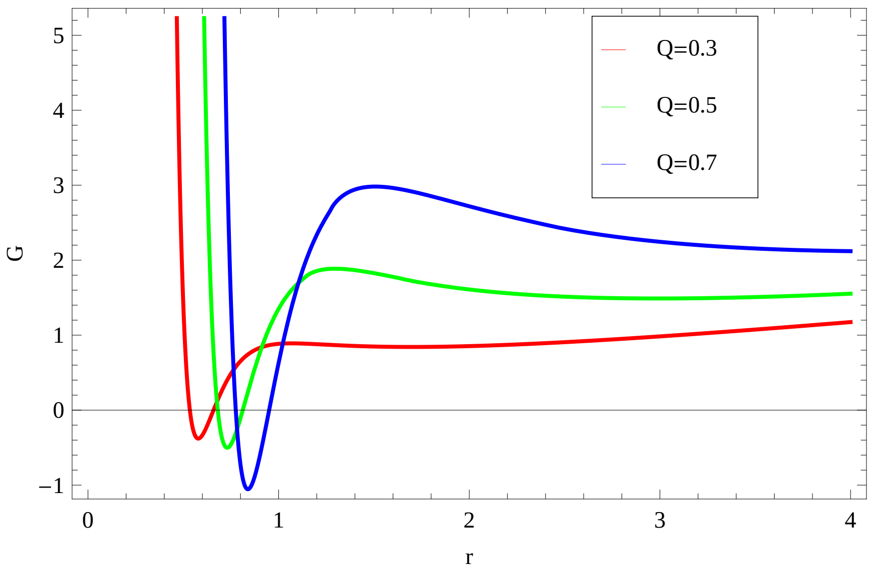

Figure 3.4: Gibb's free energy in terms of horizon radius.

3.3.1 Grand Canonical Ensemble

The free energy in grand canonical snsemble is called Gibb's free energy. Gibb's free energy can be used to determine the small/large BH phase transition . Gibb's free energy is define as

$$\begin{aligned} G &= M - TS \qquad (3.3.5)\\ G &= \frac{10r^6 + 5\kappa Q^2 r^4 - 2\kappa\alpha Q^4}{20r^5} - \left(\frac{10r^6 - 5\kappa Q^2 r^4 + 10\kappa\alpha Q^4}{40\pi r^7}\right) \\ &\times \left(\pi r^2 - (\frac{b}{2})\ln[\frac{(10r^6 - 5\kappa Q^2 r^4 + 10\kappa\alpha Q^4)^2}{(40)^2\pi r^{12}}]\right). \qquad (3.3.6) \end{aligned}$$

We observe from the **Fig.3.4** that Gibb's free energy is maximum at $r = 1.4$ due to logarithmic correction terms. it is clear that logarithmic correction can also decrease Gibb's free energy. We notice that at $Q = 0.7$ Gibb's free energy is greater than the energy at $Q = 0.3, 0.5$. We see that the free energy is globally stable when $r > 1.2$. It is interesting that Gibb's free energy becomes negative in the range of 0.5< $r < 0.9$. At that phase

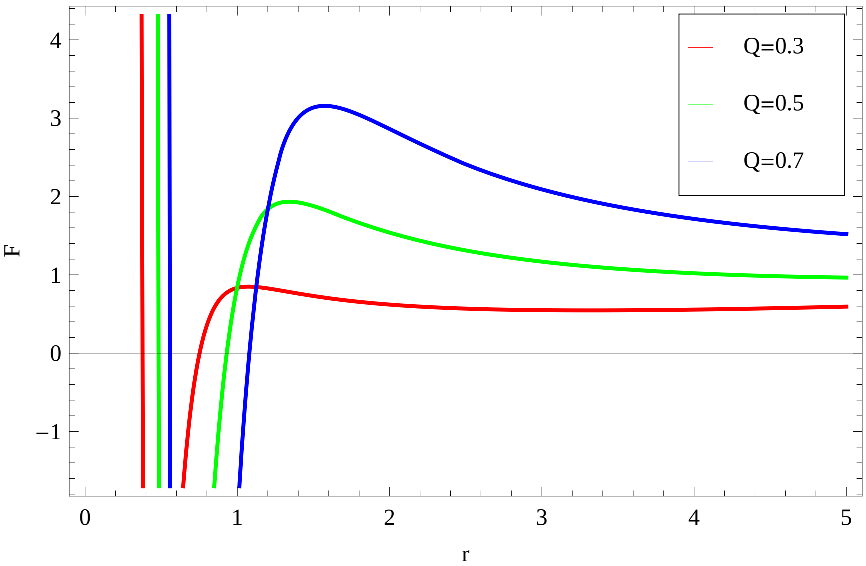

Figure 3.5: Helmholtz free energy in terms of horizon radius.

transition, Gibb's free energy is unstable. If the value of Q is higher then free energy become more stable.

3.3.2 Canonical Ensemble

The free energy in the canonical ensemble is known as the Helmholz free energy. To find this energy we can use Gibb's free energy, pressure and volume given in Eq. (3.1.4), (3.2.3) and (3.3.6).

$$F = G - PV \tag{3.3.7}$$

$$= \frac{1}{(240\pi r^7)}\Big(2\pi r^8 + 2Q^2\big(\pi r^2(55r^4 - 62Q^2\alpha) + 10b(r^4 - 6Q^2\alpha)\big)\kappa + 15b(2r^6 - Q^2r^4\kappa + 2Q^4\alpha\kappa)\ln[\frac{(2r^2 - Q^2r^4\kappa + 2Q^4\alpha\kappa)^2}{64\pi r^{12}}]\Big). \tag{3.3.8}$$

From the **Fig.3.5** we see that logarithmic correction term reduce the Helmholtz free energy. The free energy first negative at the radius horizon of 0.5< r <1 and unstable but after that it increases. The Helmholtz free energy is maximum at $r = 1.5$. The free energy for $Q = 0.7$ is high then $Q = 0.3, 0.5$. As the horizon radius increases the free energy remains constant.

Chapter 4

Thermodynamics of Janis-Newman-Winicour Space-Time and Fragmentation of $f(R)$ Global Monopole

In this chapter, we consider BH and obtain thermodynamic quantities like entropy, pressure, specific heat, Gibb's free energy and Helmholtz free energy in the presence of thermal fluctuation. We check the stability of black hole. We also discuss the phase transition of BH and check local and global stability of BH.

4.1 Janis-Newman-Winicour Space-Time

The Janis-Newman-Winicour (JNW) solution gets as an extension of Schwarzschild space-time when a scalar massless field (with vanishing potential) is introduced. This is not a vacuum solution reference. Hence the singularity coordinates in the Schwarzschild space-time come to be a naked singularity in JNW space-time. There are several astrophysical aspect distinguishing a BH from a naked singularities. Moreover gravitational lensing features have also been explored because of naked singularities[33, 34]. In literature many forms of JNW metric is available but we adopt the following form [35].

$$A(r) = \left[\frac{2r - r_0(\mu-1)}{2r + r_0(\mu-1)}\right]^{\frac{1}{\mu}}, \tag{4.1.1}$$

where μ is scalar charge which define in the interval $(1, \infty)$, and r_0 is related to mass by $r_0 = 2M$. By solving Eq.(4.1.1) and take $A(r) = 0$, we get

$$M = \frac{r}{\mu - 1}. \tag{4.1.2}$$

The temperature and entropy for this BH become

$$T = -\frac{r_0(-1 + \frac{2(r_0+2r)}{r_0+2r+r_0\mu})^{\frac{1}{\mu}}}{-\pi(b+2r)^2 + r_0^2\pi\mu^2}, \tag{4.1.3}$$

$$S = \pi r^2 - \frac{1}{2} b \ln\left[\frac{r_0^2 r^2(-1 + \frac{2(r_0+2r)}{r_0+2r+r_0\mu})^{\frac{2}{\mu}}}{\pi((r_0+2r)^2 - r_0^2\mu^2)^2}\right]. \tag{4.1.4}$$

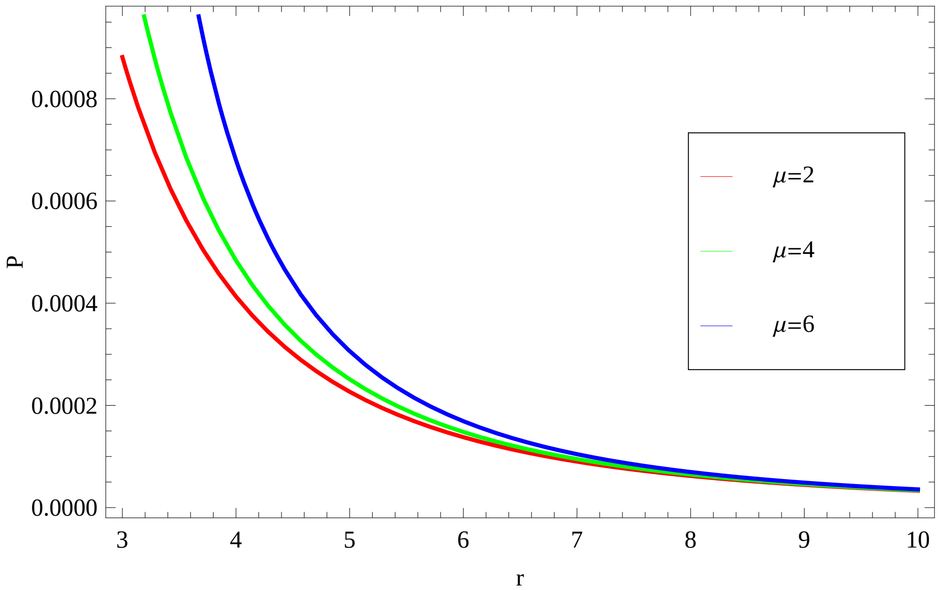

Figure 4.1: Plot of pressure versus horizon radius.

We can find the pressure from Eq. (3.1.4), (4.1.3) and (4.1.4)

$$\begin{aligned} P &= r_0(-1+\frac{2(r_0+2r)}{r_0+2r+r_0\mu})^{\frac{1}{\mu}}(4r^2(+2\pi r^2)+r_0(-4br+8\pi r^3) \\ &+ r_0^2(b-2\pi r^2)(-1+\mu^2))(4\pi^2 r^3(r_0+2r-r_0\mu)^2 \\ &\times (r_0+2r+r_0\mu)^2)^{-1}. \end{aligned} \tag{4.1.5}$$

From the **Fig.4.1** we discuss the pressure for three values of μ where $b=1$ and $r_0=1$. We notice that the value of pressure is maximum at $r=3.2$. We observe that the graph of pressure decreases due to logarithmic correction terms. It is interesting to note that the graph of pressure decreases as the range of horizon radius are increases.

4.1.1 Stability and Phase Transition

Using Eq. (4.1.2) and (4.1.3) specific heat under constant pressure becomes

$$C_P = -\frac{\pi((r_0+2r)^2-r_0^2\mu^2)^2\left(-1+\frac{2(r_0+2r)}{r_0+2r+r_0\mu}\right)^{\frac{1}{\mu}}}{8r_0 r(\mu-1)}. \tag{4.1.6}$$

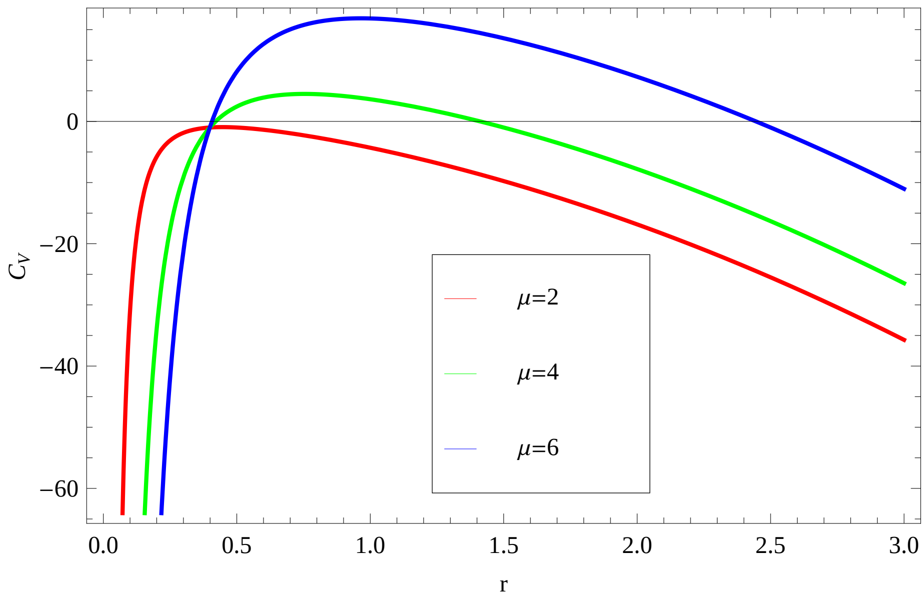

Figure 4.2: Specific heat at constant volume versus horizon radius.

We determine the value of C_V by using Eq. (4.1.3), (4.1.4)

$$\begin{aligned} C_V &= -\frac{1}{8r^2}(4r^2(b+2\pi r^2)+r_0(-4br+8\pi r^3)+(r_0)^2 \\ &\times (b-2\pi r^2)(-1+\mu^2)8r^2). \end{aligned} \tag{4.1.7}$$

From the **Fig.4.2** we see that the values of C_V first increase and after some time it decreases due to the logarithmic correction. We notice that when $\mu = 4$ the range of horizon radius for local stability is $0.4 < r < 1.5$. It is interesting to note that the local stability for $\mu = 6$ and the range of horizon radius is $0.4 < r < 2.4$. The range of horizon radius for un stability at $\mu = 4$ is $1.5 < r < 3$ and range for $\mu = 6$ is $2.5 < r < 3$. We note that when $\mu = 2$ the value of C_V is locally unstable for all values or horizon radius. Furthermore, we can find the critical point for phase transition. The critical point for $\mu = 4$ is $r = 1.5$. The point for $\mu = 6$ is $r = 2.5$. We note that critical point of $\mu = 4$ is near to BH.

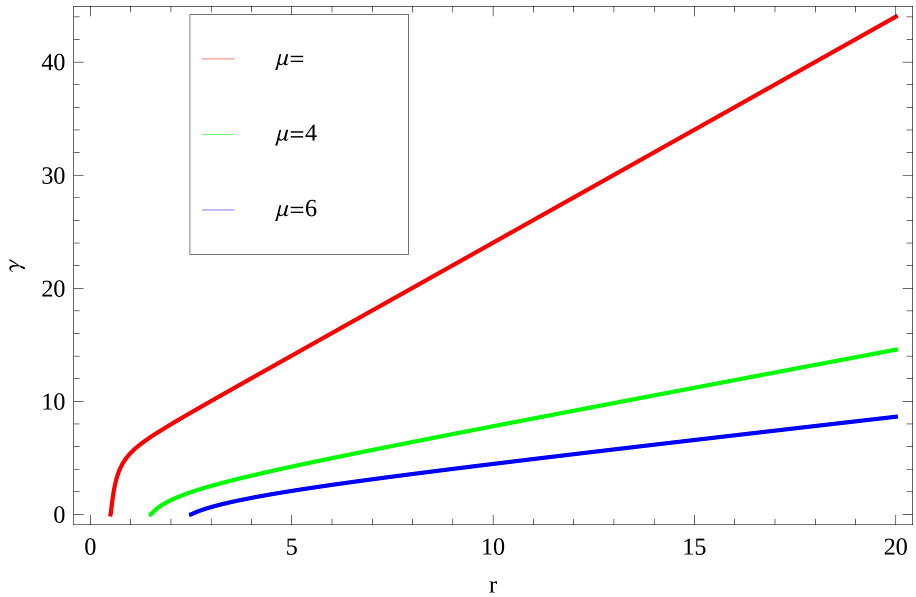

Figure 4.3: γ verses horizon radius.

The value of $\gamma = C_P/C_V$ yields

$$\begin{aligned} \gamma &= \pi r((r_0+2r)^2 - r_0^2\mu^2)^2\left(-1+\frac{2(r_0+2r)}{r_0+2r+r_0\mu}\right)^{\frac{1}{\mu}} \\ &\times \Big(r_0(-1+\mu)(4r^2(b+2\pi r^2)+r_0(-4br+8\pi r^3) \\ &+ r_0^2(b-2\pi r^2)(-1+\mu^2))\Big)^{-1}. \end{aligned} \quad (4.1.8)$$

From the **Fig. 4.3** we see the value of γ is maximum for $\mu = 2$ and $\gamma \to 50$. For $\mu = 4$ the $\gamma \to 10.3$. It is interesting to note that as we increase the value value of r the values of γ are also increase. We observe that the graph is stable for all three values of μ.

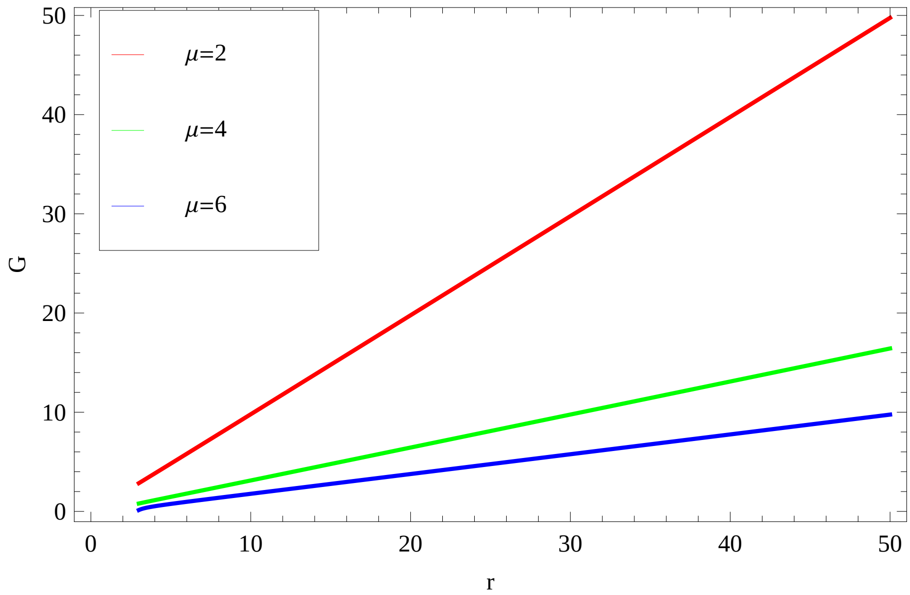

Figure 4.4: Gibb's free energy in terms of horizon radius.

4.1.2 Grand Canonical Ensemble

By using Fq.(4.1.2), (4.1.3) and (4.1.4) the Gibb's free energy is define as

$$G = \frac{b\left(-1+\frac{2(r_0+2r)}{r_0+2r+r_0\mu}\right)^{\frac{1}{\mu}}\left(2\pi r^2 - b\ln\left[\frac{(r_0)^2r^2(-1+\frac{2(r_0+2r)}{r_0+2r+r_0\mu})^{\frac{1}{\mu}}}{\pi((r_0+2r)^2-(r_0)^2\mu^2)^2}\right]\right)}{-2\pi(r_0+2r)^2+2(r_0)^2\pi\mu^2} + \frac{r}{\mu-1}. \tag{4.1.9}$$

From the **Fig. 4.4** , we see the behavior f Gibb's free energy for three values of μ. It is interesting to see that Gibb's free energy is maximum when $\mu = 2$ then $G \to 50$ and minimum for $\mu = 4, 6$ the range of $G \to 10.3$. We observe that for all values of μ the free energy is locally stable.

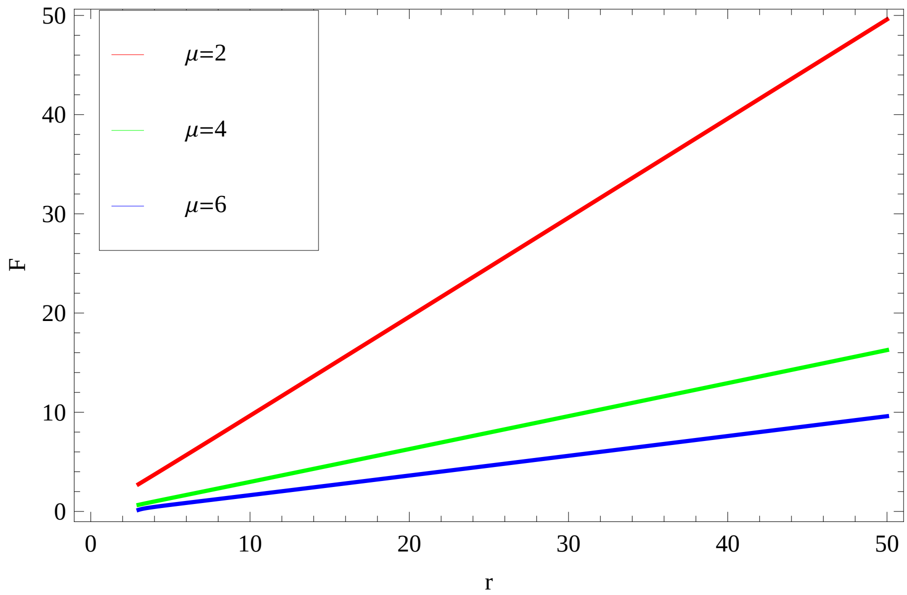

Figure 4.5: Helmholtz free energy in terms of horizon radius.

4.1.3 Canonical Ensemble

The Hlmholtz free energy is determine from Eq. (3.1.4), (4.1.5) and (4.1.9)

$$
\begin{aligned}
F &= -\frac{b}{(3\pi((r_0+2r)^2 - r_0^2\mu^2)^2)}\left(-1+\frac{2(r_0+2r)}{r_0+2r+r_0\mu}\right)^{\frac{1}{\mu}} \\
&\times \left(4r^2(b+2\pi r^2) + r_0(-4br+8\pi r^3) + r_0^2(b-2\pi r^2)(-1+\mu^2)\right) \\
&+ \frac{r}{\mu-1} + \frac{r_0}{(-2\pi(r_0+2r)^2 + 2r_0^2\pi\mu^2)}\left(-1+\frac{2(r_0+2r)}{r_0+2r+r_0\mu}\right)^{\frac{1}{\mu}} \\
&\times \left(2\pi r^2 - c\ln[\frac{r_0^2 r^2(-1+\frac{2(r_0+2r)}{r_0+2r+r_0\mu})^{\frac{2}{\mu}}}{\pi((r_0+2r)^2 - r_0^2\mu^2)^2}]\right).
\end{aligned} \tag{4.1.10}
$$

We observed from the **Fig.4.5** that Helmholtz free energy is maximum at $\mu = 2$ and $F \to 50$. When $\mu = 4$ the $F \to 10.4$ and for $\mu = 6$ the $F \to 10$. We see that the values of free energy are increases as the range of horizon radius is increase .

4.2 The Fragmentation of a Black Hole with a $f(R)$ Global Monopole

We discuss the entropy of BH with global monopole in the $f(R)$ gravity. The spherically symmetric metric was define in [35, 36]

$$ds^2 = A(r)dt^2 - B(r)dr^2 - r^2(d\theta^2 + \sin^2\theta d\varphi^2). \tag{4.2.1}$$

Where

$$A(r) = 1 - 8\pi G\eta^2 - \frac{2GM}{r} - \psi_0(r), \tag{4.2.2}$$

G is Newtonian constant. η is monopole parameter of the order 10^6 GeV in a typical grand unified theory, and $8\pi G\eta^2 \approx 10^{-5}$ [37]-[40]. M is the mass parameter. The factor ψ_0 indicate the extension of Einstein's general relativity.

According to $A(r) = 0$ we will obtain the value of M

$$M = -\frac{r(-1 + 8G\pi\eta^2 + r\psi_0)}{2G}. \tag{4.2.3}$$

The temperature and entropy of BH is

$$\begin{aligned} T &= \frac{2GM - r^2\psi_0}{4\pi r^2} & (4.2.4)\\ S &= \pi r^2 - \frac{1}{2}b\ln[\frac{r^2(\frac{2GM}{r^2} - \psi_0)^2}{16\pi}]. & (4.2.5)\end{aligned}$$

The value of P can be obtained by using Eqs.(3.1.4), (4.2.4) and (4.2.5).

$$P = \frac{2hM(b + 2\pi r^2) + r^2(b - 2\pi r^2)\psi_0}{16\pi^2 r^5}. \tag{4.2.6}$$

From the **Fig.4.6** we determine the pressure by using three values Of ψ_0 where $b = 1$, $8G\pi\eta^2 = 10^{-5}$ and $h = 1$. We see that the values of p are decreasing due to logarithmic correction terms. As we increase the range of r the values are decreases. At $r = 8$ the graph is approaches to zero.

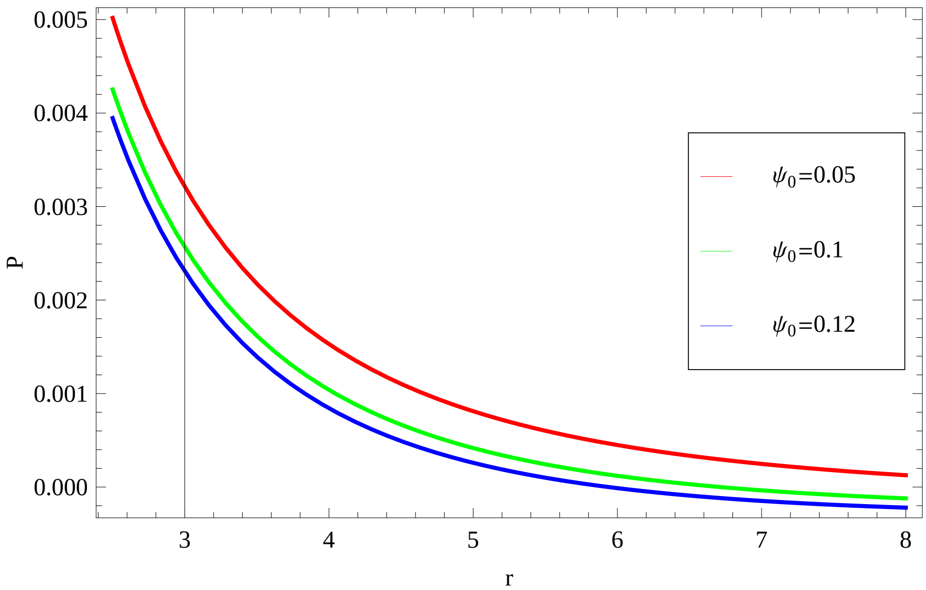

Figure 4.6: Plot of pressure versus horizon radius.

4.2.1 Stability and Phase Transition

The expressions for C_V and C_P are

$$C_V = \frac{-2hM(b+2\pi r^2)+(-br^2+2\pi r^4)\psi_0}{4hM}. \tag{4.2.7}$$

From the **Fig. 4.7** we see that the range of horizon for local stability at $\psi_0 = 0.12$ is $6 < r < 8$ and local stability for $\psi_0 = 0.1$ the range of radius horizon is $6.9 < r < 8$. The $\psi_0 = 0.05$ is unstable for all values of r .We see that the range of horizon radius for $\psi_0 = 0.05$ is greater then $\psi_0 = 0.12$. The critical point for phase transition at $\psi_0 = 0.1$ is $r = 6.8$ and critical point for $\psi_0 = 0.12$ is $r = 6$. It is interesting to see that the critical point for $\psi_0 = 0.12$ is near to BH.

The value of C_P is obtained by using the Eq. (4.2.3) and (4.2.4)

$$C_P = \frac{2\pi r^2(-1+\frac{2r\psi_0}{1-8h\pi\eta^2})}{h}, \tag{4.2.8}$$

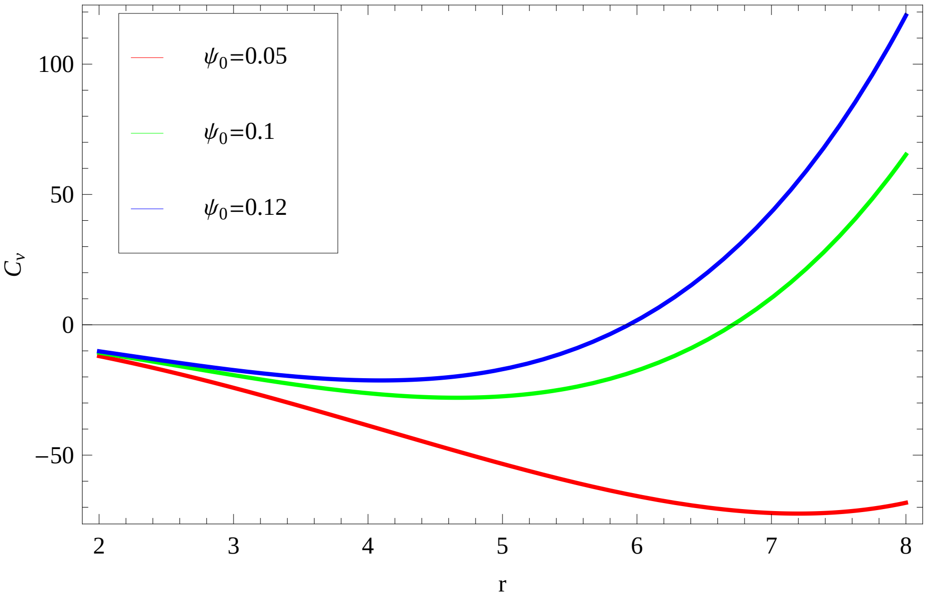

Figure 4.7: Plot of pressure versus horizon radius.

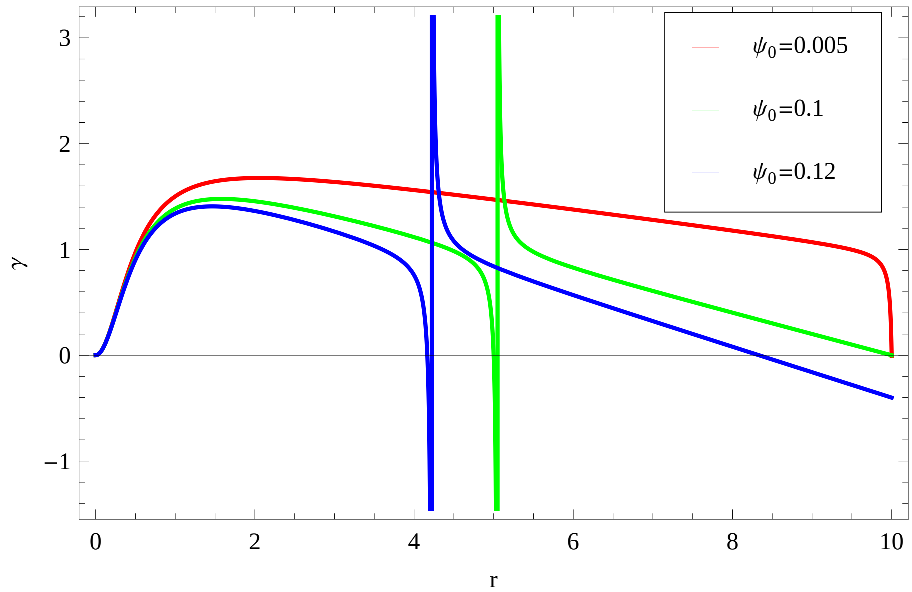

Figure 4.8: Plot of pressure versus horizon radius.

whereas

$$\gamma = \frac{4\pi r^2(-1+8h\pi\eta^2+r)\psi_0(-1+8h\pi\eta^2+2r\psi_0)}{h(-1+8h\pi\eta^2)((b+2\pi r^2)(-1+8h\pi\eta^2)+4\pi r^3\psi_0)}. \quad (4.2.9)$$

We see from the **Fig. 4.8** that first the value of γ increases and after some time the value decreases. The value os γ is maximum when $\psi_0 = 0.05$ at $r = 1.5$ and $\gamma \to 1.6$. The values of γ are decreasing due to logarithmic correction terms. The value of γ is minimum for $\psi_0 = 0.12$ when $r = 1.5$ and $\gamma \to 1.4$. When $\psi_0 = 0.05$ the γ is stable when $0 < r < 10$. For $\psi_0 = 0.1$ the range of horizon radius for stable is $0 < r < 4$ and $5.5 < r < 10$. The range for stability of $\psi_0 = 0.12$ is $0 < r < 4$ and $4.5 < r < 8$. The graph shows an unstable for all three values of ψ_0 when $10 < r < 0$.

4.2.2 Grand Canonical Ensemble

Gibb's free energy is determine by using the value of M, T and S

$$\begin{aligned} G &= (2\pi r^2 + b\ln[16\pi] - b\ln[(-1+8h\pi\eta^2+2r\psi_0)^2] \\ &\times \frac{(-1+8h\pi\eta^2+2r\psi_0))}{(8\pi r)} - \frac{r(-1+8h\pi\eta^2+r\psi_0)}{2h} \end{aligned} \quad (4.2.10)$$

From above graph **Fig. 4.9** we see that as we increase the value of r the value of Gibb's free energy is also increases. All the three values of ψ_0 achieve their maximum at the same value of $r = 4$. The Gibb's free energy is unstable when $0.6 < r < 0.9$. After that the graph become stable for greater range of horizon radius.

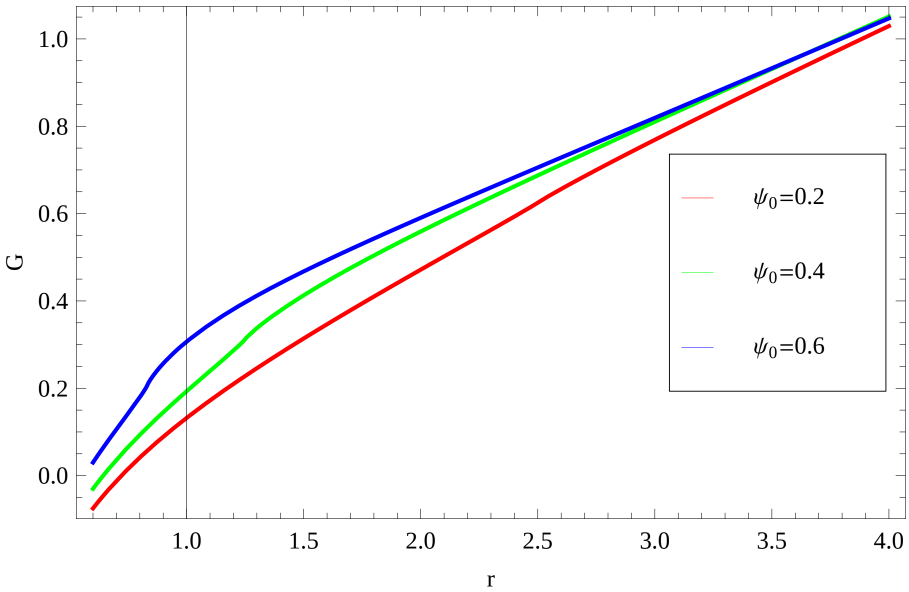

Figure 4.9: Plot of pressure versus horizon radius.

4.2.3 Canonical Ensemble

By us Eq. (3.1.4), (4.2.6) and (4.2.10) the Helmholtz free energy is define as

$$\begin{aligned} F &= \frac{1}{24h\pi r}\Big((-1+8h\pi\eta^2)(2(-6+5h)\pi r^2 + bh(2+3\ln[16\pi]) \\ &- 3bh\ln[(-1+8h\pi\eta^2+2r\psi_0)^2]) + 2r(2(-3+5h)\pi r^2 \\ &+ 3bh\ln[16\pi] - 3bh\ln[(-1+8h\pi\eta^2+2r\psi_0)^2]\psi_0\Big). \end{aligned} \tag{4.2.11}$$

Farom the **Fig. 4.10** we see that the free energy is increases as we increase the value of r. We see that the free energy is maximum when $F \to 14$ for $\psi_0 = 0.12$ and $r = 18$. It is interesting to see that the free energy is minimum when $F \to 6.5$ for $\psi_0 = 0.05$ and $r = 18$. We observe that the free enegy is increases as we increase the value of ψ_0 and value of event horizon.

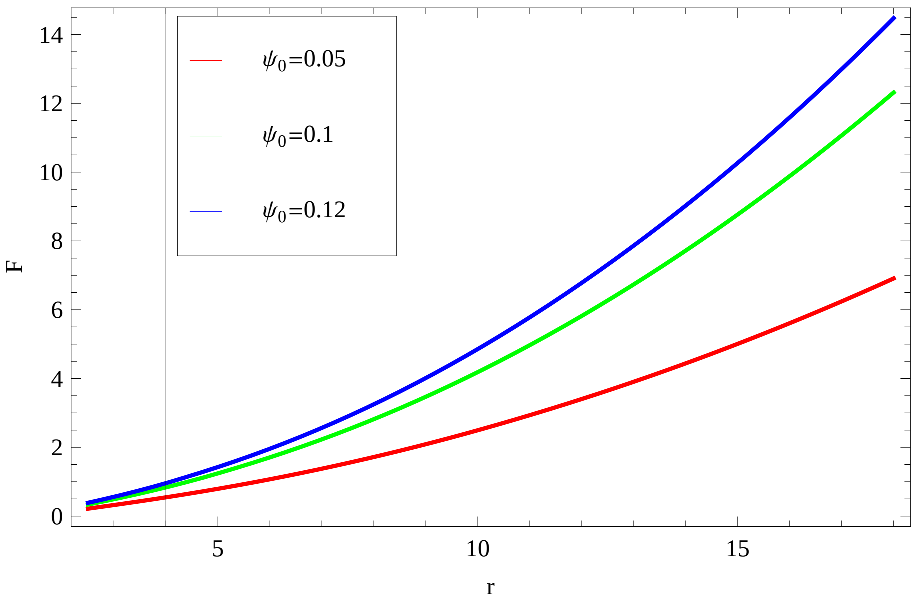

Figure 4.10: Plot of pressure versus horizon radius.

Chapter 5

Conclusion

In this thesis, we have discussed the effect of thermal fluctuation on DSRN, JWN and fragmentation of BH with a $f(R)$ global monopole. We have calculated the mass, entropy and temperature. By using these terms, we have studied the effect of thermal fluctuation on BHs. We have also used the logarithmic correction of entropy and discussed the behavior of pressure and specific heat. We have observed that the pressure decreases due to logarithmic correction in RN, JNW and $f(R)$ global monopole.

We have also determined the ratio of specific heat under constant volume and pressure (γ), we noticed that for RNBH the value of γ is stable for large horizon and it becomes unstable for small horizon radius. In JNW BH, the value of γ is stable for for large horizon radius and for BH of $f(R)$ global monopole the value of γ is unstable for large and small range of horizon radius. We have also determine the phase transition for three BHs. We see that in RN and $f(R)$ global monopole BH the graph is stable for greater range of horizon radius and in JNW BH the graph is unstable for higher values of horizon radius.

We also investigated the Gibb's free energy and Helmholtz free energy. We see that the free energy is induced in the presence of logarithmic correction terms. It is notice that in all the three BHs the free energy is stable as we increase the values of constants. The graph of free energy is increasing as we increase the value of horizon radius. We noticed that RN, JNW and $f(R)$ global monopole BHs are locally and globally stable.

Bibliography

[1] J. D. Bekenstein: Lett. Nuovo Cimen. **4**(1972)737.

[2] J. D. Bekenstein: Phys. Rev. D **7**(1973)2333.

[3] J. M. Bardeen, B. Carter and S. W. Hawking: Commun. Math. Phys. **31**(1973)161.

[4] S. W. Hawking: Nature **248**(1974)30.

[5] J. D. Bekenstein: Phys. Rev. D **9**(1974)3292.

[6] S. W. Hawking: Commun.Math.Phys. **43**(1975)199.

[7] S. W. Hawking and D. N. Page: Commun.Math.Phys. **87**(1983)577.

[8] P. K. Townsend: arXiv:gr-qc/9707012.

[9] R. M. Wald: Liv. Rev. Relativ. **4**(2001)1.

[10] D. N. Page: New J. Phys. **7**(2005)203.

[11] S. W. Hawking: Nature **248**(1974)30. .

[12] S. W. Hawking: Commun. Math. Phys. **43**(1975)199.

[13] N. Altamirano, D. Kubiznak, R. B. Mann, and Z. Sherkatghanad: Galaxies **2**(2014)89.

[14] D. Bak and S. J. Rey: Class. Quant. Grav. **17**(2000)L1.

[15] S. K. Rama: Phys. Lett. B **457**(1999)268.

[16] A. Ashtekar: *Lectures on Non-perturbative Canonical Gravity*, (World Scientific, 1991).

[17] T. R. Govindarajan, R. K. Kaul, V. Suneeta: Class. Quant. Grav. **18**(2001)2877.

[18] S. Carlip: Class. Quant. Grav. **17**(2000)4175.

[19] R.B. Mann, S.N. Solodukhin: Nucl. Phys. B **523**(1998)293.

[20] A.J.M. Medved, G. Kunstatter: Phys. Rev. D **60**(1999)104029.

[21] A.J.M. Medved, G. Kunstatter: Phys. Rev. D **63**(2001)104005.

[22] T. R. Govindarajan, R. K. Kaul and V. Suneeta: Class. Quant. Grav. **18**(2001)2877.

[23] D. Birmingham and S. Sen: Phys. Rev. D **63**(2001)47501.

[24] V. K. Oikonomou: Universe **2**(2016)10.

[25] S. P. Kim, H. K. Le, Y. Yoon: arXiv:1503.00218v1.

[26] B. Chen, J. Zhang: arXiv:1212.1959v2.

[27] S. Roy, A. K. Sen: arXiv:1508.01429v3.

[28] T. Karmakar, T. Sarkar: arXiv:1709.08935v2.

[29] S. Zhou, R. Zhang, J. Chen, Y. Wang: arXiv:1408.6041v1.

[30] J. Man, H. Cheng: 1301.2739v1.

[31] L. Chen, H. Cheng: arXiv:1607.07138v2.

[32] L. Chen, H. Cheng: Eur. Phys. J. C **78**(2018)196.

[33] K. S. Virbhadra, G. F. R. Ellis: Phys. Rev. D **65**,103004(2002).

[34] K. S. Virbhadra, D. Narasimha, S. M. Chitre: Astron. Astrophys. **337**,1 (1998)

[35] A. N. Chowdhury, M. Patil, D. Malafarina, P. A. Joshi: Phys. Rev. D **85**,104031 (2012).

[36] T. R. P. Carames, E. R. B. de Mello, M. E. X. Guimaraes: Int. J. Mod. Phys. Conf. Ser. **03**, 446 (2011).

[37] T. R. P. Carames, E. R. B. de Mello, M. E. X. Guimaraes: Mod. Phys. Lett. A **27**, 1250177 (2012).

[38] A. Vilenkin: Phys. Rep. **121**, 263 (1985).

[39] T. P. Cheng, L. F. Li: *Gauge Theory of Elementary Particle Physics* (Clarendon Press, Oxford, 1984).

[40] M. Barriola, A. Vilenkin: Phys. Rev. Lett. **63**, 341 (1989).